Environmental Science Nano

ROYAL SOCIETY OF CHEMISTRY

PAPER

View Article Online
View Journal | View Issue

Cite this: *Environ. Sci.: Nano*, 2020, 7, 1742

Fragmentation of polymer nanocomposites: modulation by dry and wet weathering, fractionation, and nanomaterial filler†

Richard Zepp, ‡[a] Emmanuel Ruggiero, ‡[b] Brad Acrey,[ac] Mary J. B. Davis,[ad] Changseok Han,[cef] Hsin-Se Hsieh,[ad] Klaus Vilsmeier,[b] Wendel Wohlleben[b] and Endalkachew Sahle-Demessie *[e]

In recent years, an increasing number of polymeric composites incorporating engineered nanomaterials (ENMs) have reached the market. Such nano-enabled products (NEPs) present enhanced performance through improved mechanical, thermal, UV protection, electrical, and gas barrier properties. However, little is known about how environmental weathering impacts ENM release, especially for high-tonnage NEPs like kaolin products, which have not been extensively examined by the scientific community. Here we study the simulated environmental weathering of different polymeric nanocomposites (epoxy, polyamide, polypropylene) filled with organic (multiwalled carbon nanotube, graphene, carbon black) and inorganic (WS_2, SiO_2, kaolin, Fe_2O_3, Cu-phthalocyanines) ENMs. Multiple techniques were employed by researchers at three laboratories to extensively evaluate the effect of weathering: ultraviolet-visible spectroscopy (UV-vis), Fourier transform infrared spectroscopy (FTIR), optical microscopy, contact angle measurements, gravimetric analysis, analytical ultracentrifugation (AUC), transmission electron microscopy (TEM), scanning electron microscopy (SEM) and Raman spectroscopy. This work aimed to elucidate the extent to which weathering protocol (*i.e.* wet *vs.* dry) and diverse filler characteristics modulate fragment release and polymer matrix degradation. In doing so, it expanded the established NanoRelease protocol, previously used for analyzing fragment emission, by evaluating two significant additions: (1) simulated weathering with rain events and (2) fractionation of sample leachate prior to analysis. Comparing different composite materials and protocols demonstrated that the polymer matrix is the most significant factor in NEP aging. Wet weathering is more realistic than dry weathering, but dry weathering seems to provide a more controlled release of material over wet. Wet weathering studies could be complicated by leaching, and the addition of a fractionation step can improve the quality of UV-vis measurements.

Received 29th November 2019,
Accepted 4th May 2020

DOI: 10.1039/c9en01360a

rsc.li/es-nano

Environmental significance

An increasing number of polymeric composites incorporating nanomaterials (NMs) has reached the market. However, the knowledge on the impacts of environmental weathering on the degradation of composites and the release of NMs is still limited, especially for high-tonnage nano-enabled materials (NEP) like kaolin products. Rigorous techniques were used to evaluate the effects of weathering, including ultraviolet-visible spectroscopy (UV-vis), Fourier transforms infrared spectroscopy (FT-IR), optical microscopy, contact angle measurements, gravimetric analysis, analytical ultracentrifugation (AUC), transmission electron microscopy (TEM), scanning electron microscopy (SEM) and Raman spectroscopy. This study expanded the NanoRelease protocols for analytical techniques, such as the difference between dry and wet weathering, that are needed for generating data for the are vital for risk analysis.

[a] *U.S. Environmental Protection Agency (EPA), Office of Research and Development (ORD), Center for Environmental Measurement and Modeling (CEMM), 960 College Station Rd., Athens, GA, USA*
[b] *BASF SE, Dept. Material Physics and Analytics, 67056, Ludwigshafen, Germany*
[c] *ORISE Research Fellow, Oak Ridge Institute for Science and Education (ORISE), Oak Ridge, TN 37830, USA*
[d] *NRC Post-Doctoral Fellow, National Research Council (NRC), Washington DC, USA*
[e] *EPA, ORD, Center for Environmental Solutions and Emergency Response (CESER), Cincinnati, OH, USA. E-mail: Sahle-Demessie.Endalkachew@epa.gov*
[f] *Department of Environmental Engineering, INHA University, Incheon, Korea*

† Electronic supplementary information (ESI) available: Details on environmental aging of polymer nanocomposites, AUC-RI, ATR-FTIR, EDX, Raman spectroscopy, release rate calculations, and quantification and characterization of released particles (*via* TEM, UV-vis, *etc.*) are included in the ESI. Additional techniques (ICP-MS, dynamic light scattering) were attempted to characterize released particles, but challenges in sensitivity limitations of these techniques made the data unreliable; results from these techniques are also discussed briefly in the ESI. See DOI: 10.1039/c9en01360a

‡ These authors contributed equally to this work.

1. Background and introduction

Nanocomposites, nano-enabled products (NEP) in which engineered nanomaterials (ENMs) are embedded in a material matrix, are ubiquitously used as construction materials, light-weight automotive parts, coatings, packaging and electronic components, and more.[1] Recently, several countries, including France and the USA, developed mandatory reporting requirements for materials that are produced or imported in nanoform.[2,3] The publicly available reports[2] highlight that for some materials, including carbon black (CB) and silica (SiO_2), almost all grades are considered nanomaterials.[4] The specific toxicity of these conventional ENMs to environmental species is low, but production quantities on the order of megatons per year warrant consideration of their release in their environmental risk characterization.[5–7] Kaolin and calcium carbonate reach an equally high level of total production quantities. Still, only a fraction was reported to be in nanoform.[2,4] Its platelet shape differentiates kaolin from other inorganic fillers and enables specific applications for high-temperature-stable polymers or for barrier polymers.

Environmental weathering, or aging, has been shown to degrade polymers through sun and rain exposure and thus constitutes a pathway toward the environmental release of nanomaterials.[8] The impacts of weathering have been assessed through artificial aging with simulated sunlight and other environmental conditions.[9] Risk screening approaches categorize nano-enabled products (NEP) by the stability of the nanocomposite structure, and assign low priority or waive further assessment on nanocomposites with a solid polymer matrix[10–12] – because the release is negligible if the polymer matrix is resilient against the conditions of intended use. However, some nanomaterials, especially CB, find commercial application as UV absorbers to stabilize polymers against weathering.[13]

Ample literature exists on the weathering, fragmentation and release of exemplary NEPs containing 0.1% to 5% of more innovative engineered nanomaterials (ENMs). The fillers into NEPs can be divided based on their shapes as particle (3D), platelet (2D) and tubular (1D) forms. Especially the one dimensional multiwalled carbon nanotubes (MWCNTs) have gained a lot of attention from the scientific community. These studies found that the polymer matrix predominantly determined the rates of aging and fragmentation, in many cases with potential for photoprotective modulation by the MWCNTs *via* UV absorption, radical scavenging, physical entanglement, or polymer crystallinity nucleation.[8,14–34]

Although different studies were conducted on CB[35,36] and SiO_2, no clear trends in weathering behavior with polymer matrix and compatibilization were observed for CB, and SiO_2 NEPs.[17,18,35,37,38] Apart from weathering, fragmentation and release studies on particle (3D) and tubular (1D) nanoforms, little is known on more industrial employed platelet (2D) fillers embedded in polymer matrix. Platelet fillers such as nanoclays (*e.g.* kaolin, montmorillonite, talc) in plastics represent high-tonnage NEPs and the most exploited NFs for automotive and packaging industries.

Although nanoclays have been traditionally used for commercial products (*e.g.* Toyota patented a nanoclay-polyamide system in 1988), are now considered to be nanomaterials, drawing more attention regarding their possible environmental impacts. To understand the extent of modulation of NEP weathering and fragmentation by the specific ENM for these high-tonnage materials, comparative testing of systematically varied NEPs must be undertaken using validated reproducible protocols.[39,40] Here, we apply the NanoRelease protocol to determine how different ENMs modulate the weathering of polymer nanocomposites. We examine the impact of weathering on the chemical and physical characteristics of a series of epoxy nanocomposites with MWCNT, SiO_2, CB, graphene (GP) fillers, thus varying shape and UV absorption of the ENM. The primary focus of this study is epoxy composites. Epoxy was selected because it is a widely used polymer for coating, structural adhesives, and composite applications. Polypropylene (PP) and polyamide (PA) were included in limited scope to provide context and points for comparison. Regarding ENM selection, GP has rarely been studied,[41] and only studies on PU and PE matrices have compared MWCNT against SiO_2 modulations.[18,35,42] In contrast to flexible MWCNT, the inorganic WS_2 nanotubes are stiff, and were earlier found to improve the shear strength, peel properties, fracture toughness and glass transition temperature of epoxy.[43] Polypropylene (PP) wafers were filled with a low concentration of nano-pigment Fe_2O_3 and Cu-phthalocyanine. We also investigated if a very high filler content of 25% kaolin in polyamide (PA), as used commercially in automotive parts, would modify the environmental fragmentation and release behavior more than in a previous release study with nanocomposites incorporating low filler contents (<5%).[44]

Beyond the previous focus on assessing the protocol's reproducibility in characterizing samples after 1000 h of irradiation, we now apply it to UV-dose-dependent aging and fragment release studies, characterizing the kinetics between 0 h and 2500 h irradiation. Two modifications to the NanoRelease protocol were evaluated for their potential to improve the accurate simulation of environmental weathering and the quality of fragment release measurements: wet aging and fractionation. Wet and dry-aging are both options of the ISO4892 standard, but they have rarely been directly compared to NEPs. Evaluation of wet aging is necessary since water may cause hydrolysis and mechanical fragmentation of some epoxy in combination with high temperatures.[37,45,46] The adsorption of water increases the diffusion coefficient of water within the polymer, and hydrolysis of polymer functional groups, such as ether linkages, can cause permanent damage to the polymer. Fractionation was accomplished by widely available methods, such as conventional centrifugation, so that future

users can assess the content of submicron fragments in the weathering-induced releases without needing access to electron microscopy. The objective of this study is to expand the previous NanoRelease protocols, and estimate the various factors affecting the environmental release of NP during the use phase and at the end of life.

2. Experimental

2.1 Study organization

Weathering studies were carried out on a series of polymer nanocomposite wafers at three separate facilities: the BASF lab in Stuttgart, Germany, the United States Environmental Protection Agency (US EPA), Center for Environmental Measurements and Modeling (CEMM) in Athens, GA, USA and the US EPA, Center for Environmental Solutions and Emergency Response (CESER) in Cincinnati, OH, USA. As in previous reports,[47] the three teams used a consistent protocol for weathering, release testing, and sample analysis that is widely acknowledged.

Good agreement was observed between UV-vis spectroscopy measurements of the released particles from the three laboratories. The demonstrated ability to replicate experiments and results between different laboratories enabled the combination of experimental data from these labs to examine samples with a wider variety of analytical techniques. In order to further characterize the released particles, analytical ultra-centrifugation (AUC) and TEM were conducted at BASF and Raman spectroscopy was conducted at EPA-CEMM. Changes in the surface chemistry and morphology of weathered wafers were examined using optical microscopy, SEM, contact angle measurements, and FTIR at EPA-CESER as well as SEM and EDX at EPA-CEMM.

2.2 Materials

Both neat (unfilled) and filled epoxy, PA and PP composites were used in this study. The epoxy used was diglycidyl ether of bisphenol A (DGEBA) with an amine curing agent. Unfilled epoxy and epoxy filled with either multiwalled carbon nanotube (MWCNT), graphene (GP), carbon black (CB), tungsten disulfide (WS_2), or silica (SiO_2) were used for this study. For epoxy-nanocomposite samples, MWCNT, GP, CB, and SiO_2 were mixed with an epoxy–amine, which was then cured to form crosslinks in 5 cm × 5 cm square molds, referred to here as "wafers". WS_2 nanotubes were tested at the same volume content in epoxy as MWCNT. PA and PP nanocomposites were respectively prepared with a high concentration of kaolin and low concentration of iron(III) oxide (Fe_2O_3) and Cu-phthalocyanine. Additionally, PA incorporates a small quantity of CB (~2% w/w). Each nanofiller was then added to its respective polymer matrix by hot-melt extrusion mixing into 5 cm × 5 cm square nanocomposites. A summary of the characteristics of each nanocomposite studied, including details on ENM fillers, is given in Table 1.

2.3 Environmental aging of polymer nanocomposites

The conditions of weathering were 60 ± 2 W m^{-2} of simulated solar irradiance in the broadband (300–400 nm) and a black-standard temperature of 65 ± 3 °C. Using an optical radiometer, we directly measured the spectral irradiance in the solar simulator at the location of the sample surface. The spectrum is included in Fig. S1 of the ESI;† the irradiance in the UV region is similar to midday solar irradiance at latitude 40 deg N during summer.[47]

As described in ISO-4892, two methods of weathering were used that will be referred to as "dry" and "wet" herein. In wet

Table 1 Supplier and material specifications of nanocomposites

Nano-composite	Polymer matrix	Polymer supplier	ENM filler	ENM supplier and grade	Filler size specifications			Filler loading (%)	
					Diameter/thickness (nm)	Length (μm)	Surface area (m^2 g^{-1})	w/w	v/v
Epoxy–MWCNT	Epoxy	University Kaiserslautern	MWCNT	Nanocyl; NC7000	10	1.5	250–300	0.38	0.22
Epoxy–GP	Epoxy	University Kaiserslautern	GP	ACS material	10	—	40	1	0.6
Epoxy–CB	Epoxy	University Kaiserslautern	CB	Ensaco; conductive grade	46	—	65	3.4	2
Epoxy–WS_2	Epoxy	University Kaiserslautern	WS_2	ApNano	30–150	1–20	—	1.5	0.22
Epoxy–SiO_2	Epoxy	University Kaiserslautern	SiO_2	Evonik; Aerosil	13	—	200	3	1.5
PA–kaolin	Polyamide (PA)	BASF SE	Kaolin	BASF SE	280	—	24	25	—
			CB	BASF SE	80	—	30	~2	—
PP–Fe_2O_3	Poly-propylene (PP)	Borealis	Fe_2O_3	Borealis	12	—	107	1	—
PP–Cu-phthalocyanine	Poly-propylene (PP)	Borealis	Cu-Phthalocyanine	BASF SE	19	—	53	0.5	—

weathering, sample wafers underwent 120 min cycles of simulated rainfall (*i.e.*, 102 min without water spraying and 18 min with water spraying), while simulated sunlight remained continuous during the cycles. Dry-aged sample wafers were continuously irradiated without the water spray cycle. EPA-CEMM and EPA-CESER implemented the wet protocol, and BASF used both the dry and wet protocols. In all cases, sample squares were placed on a stainless-steel mesh grid and held by stainless steel screws before the wafer was placed in the weathering chamber (Fig. S2 in the ESI†). The wafers in the aging chamber were rotated 180° once a week throughout the weathering process, to account for inconsistent sample exposure to spraying.

Wet cycles were repeated and dry-aging continued until total weathering time reached 1000 h for epoxy samples or 2500 h for polyamide and polypropylene samples in all three laboratories. In addition, EPA-CESER aged subsets of their epoxy samples to 500 h and 2500 h and their PA samples to 1000 h in order to provide information on kinetic trends.

2.4 Physical characterization of material surfaces

SEM and optical microscopy were used to investigate the surface morphology of aged and unaged samples and visualize the extent of weathering. Optical images were collected with a Keyence VHX-600 digital microscope (Keyence Corp. of America). A JEOL JSM 6490LV scanning electron microscope (JSM6490V) was used at a voltage of 3–5 kV. Contact angles of water on pristine and aged samples were measured with a drop shape analyzer (DSA25E, KRÜSS GmbH).

2.5 Attenuated total reflectance Fourier transform infrared spectroscopy (ATR-FTIR)

Attenuated total reflectance Fourier transform infrared (ATR-FTIR) spectroscopy was used to analyze changes of the molecular structure and functional groups in the surface of the unfilled and filled epoxy composites. ATR-FTIR can identify carbonyl groups such as ketones, carboxylic acids, and aldehydes.[48] The carbonyl index (CI), defined as the ratio of the peak height of the carbonyl at 1712 cm^{-1} to the peak height at 1465 cm^{-1}, was used as a parameter to monitor the degree of photo-oxidation of epoxy.[49]

2.6 Collection of released fragments and nanomaterials

Released polymer fragments and nanomaterials were investigated upon weathering by placing sample wafers in glass jars with 25 mL of MilliQ water acting as a leaching medium. Dark control wafers were kept in a laboratory drawer and added to glass jars upon the conclusion of weathering. All labs implemented the same weathering protocol and subsequent leaching step, as well as sonication post-weathering. For sonication, BASF used a Bandelin Sonorex Digital 10P at 720 W and 35 kHz for 1 h, EPA-CEMM used Branson M5800 160 W and 40 kHz for 1 h, and EPA-CESER used a Cole-Parmer 750 W horn sonicator for 5 minutes. Once the leachates were extracted from the jars, we noticed that there were particles that had settled to the bottom of our test tubes. Samples were treated with surfactant, sodium dodecyl sulfate (SDS), and had either 1% SDS in the case of BASF and EPA-CESER, or 0.1% SDS for EPA-CEMM. This addition also required further sonication with the use of sonicator probes (BASF: Branson Sonifier® SFX550, 550 W, 20 kHz for 30 s; EPA-CEMM: Sonics Vibracell probe, 100 W, 20 kHz for 1 h; EPA-CESER: Cole Parmer 750 W horn probe for 15 min) to promote better dispersion of fragments. After sonication, the samples were fractionated using a tabletop centrifuge (1 h, 1000 rpm, r = 7.5 cm). The supernatants were collected and concentrated after discarding the pellets. Bubbling down nitrogen, sample volume was reduced to 2.5 mL for BASF and EPA-CESER and 4.5 mL for EPA-CEMM. The energy expended during these sonication procedures equals the cross-product of power (Watt), which varied between the labs: BASF 2.6×10^6 joules, EPA-CEMM 5.8×10^5, and EPA CESER 2.2×10^5. This analysis suggests that BASF expended much more energy during sonication than the two EPA labs. Because the power density of sonication is proportional to sonochemical degradation kinetics of organic materials, potentially including carbon nanomaterials[50] and epoxy fragments, the differences potentially could have affected the results.[51] However, few studies are available that could be used to quantitatively evaluate the role of sonochemistry in the present study.

2.7 Ultraviolet-visible (UV-vis) spectroscopy

UV-vis spectroscopy was performed by EPA-CEMM utilizing a Perkin Elmer Lambda 35 instrument (PerkinElmer, Inc., CT, USA). UV-vis data from BASF were measured employing an Ocean-Optics USB2000 (Ocean Optics GmbH, GER) spectrometer, and data at EPA-CESER were collected with a SpectraMax Plus (Molecular Devices, CA, USA). For all NEPs, duplicate samples were analyzed for each experimental setup (*e.g.* dry *vs.* wet, fractionation *vs.* no-fractionation). Leachate samples were scanned before and after fractionation using a 1 cm path length cell to show effects on absorbance. The raw data for the UV-vis absorption profile for the different aging times were normalized based on the absorption of a corresponding blank water sample and were reported as absorption coefficients that were normalized to cell path length. Data from leaching water samples were also compared with the peaks of freely dispersed MWCNT, graphene, and carbon black that were subjected to the same sonication and subsequent fractionation as the leachate samples. The absorption coefficients of all the fillers in the test were sufficiently significant to permit selectivity at the chosen wavelength. Other studies have demonstrated that the different forms of graphite show two major absorbance peaks that are at 223 nm and 273 nm corresponding to graphene oxide and dispersed graphene, respectively.[52] Since all specimens had significant absorption coefficients at 275 nm, coefficients at this wavelength were measured for each

sample. Intensities collected from samples at EPA-CEMM were multiplied by 1.8 to account for their difference in concentration resulting from bubbling, as described in section 2.6.

2.8 Transmission electron microscopy (TEM)

The analysis of released fragments in runoff waters was performed using FEI/Thermo Tecnai G2 transmission electron microscope at an acceleration voltage of 200 keV. The TEM samples were prepared by dropping a few μl of the sample solutions onto 300 mesh per inch copper grids with carbon film followed with the evaporation of the water. Cross-sections of the epoxy composites were prepared by ultra-microtome and were also analyzed by TEM (see Fig. S12 in the ESI†).

2.9 Raman spectroscopy

IR and Raman spectroscopic techniques have been used to study the oxidation of CNTs.[51–53] Raman analysis was performed by pipetting 30–50 μL of sample leachates onto aluminum foil-wrapped, glass slides. Aliquots of 10 μL were added and allowed to dry on the slide inside of the plastic petri dish for 8 hours. Control samples of CNT and graphene were prepared at 5 ppm concentration in MilliQ grade water and analyzed before running leachate samples for a basis of comparison. This procedure was repeated until sufficient concentration was detectable with a Renishaw inVia confocal Raman system (Renishaw PLC, United Kingdom). We utilized a single-mode, 785 nm diode module for irradiation of the sample with 10 second exposure time at power ~1 mW (0.5% of total laser power), to not oversaturate the sample. Raman shifts were measured from 100–3200 cm^{-1}. The system was calibrated using a single crystal silicon wafer with an absorption peak at 520 cm^{-1}. The glass slides were then placed inside the Raman chamber under the microscope for analysis. Under the microscope, we located the edge of the droplet(s) and focused the beam there. Each slide was analyzed at three different sample spots to check for consistency and reproducibility.

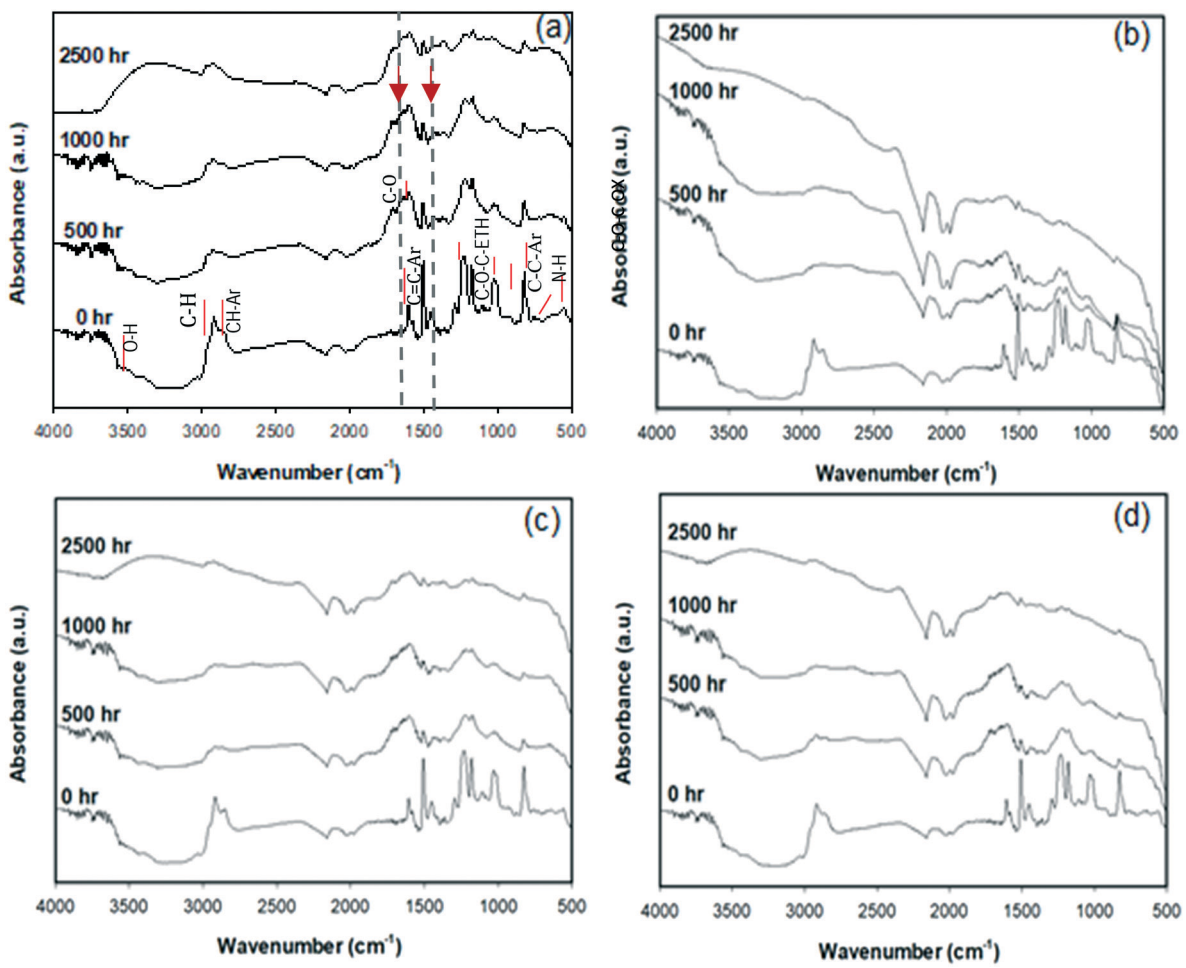

Fig. 1 ATR-FTIR spectra of (a) neat epoxy, (b) epoxy–CB, (c) epoxy–CNT, and (d) epoxy–GP composites, after 0, 500, 1000, and 2500 h of wet weathering (arrows show absorption peaks used to calculate the CI).

3. Results and discussion

3.1 Changes to surface chemistry of epoxy–NM composites by weathering

The degradation of epoxy wafers resulted in changes in the physical, chemical, and structural properties of the exposed surfaces. Amorphous polymers, such as epoxy, are particularly susceptible to aging due to easy fluid penetration through their relatively-open structure,[53] coupled with their photolabile functional groups.[54,56]

Degradation due to solar UV exposure is mainly due to C–C scission, resulting in chain fragmentation, coupled with photoreactions of side groups.[55,56] These chemical changes occurring at the surface of epoxy during weathering exposure were monitored by following the formation and disappearance of chromophoric groups using ATR-FTIR. ATR-FTIR spectra (Fig. 1) were collected from epoxy, and epoxy composites prior to weathering (0 h), and after 500, 1000 and 2500 hours of accelerated weathering. Spectra were collected at the same location on each sample and compared in terms of aging time and filler material to evaluate the overall effects of weathering and ENM identity on composite degradation.

ATR absorption peaks were identified as those associated with the chemical structure of diglycidylether of bisphenol A (DGEBA) because of the location and intensity of characteristic bands indicated in Fig. 1(a). The assignment of the spectral band was based on published work.[57] The spectra of unaged samples also exhibit IR resonances with peak positions 1608 and 1509 cm^{-1} for stretching C═C and C–C aromatic rings that are known constituents of bisphenol-A epoxy resin Brad.

As the aging period increased, most of the IR absorption peaks showed a progressive increase in absorbance and attenuation in width, as shown in Fig. 1. Changes in absorption peaks of specific features were superimposed on the across-the board increases in surface absorbance caused by changes in light scattering related to changes in surface morphology. After 500 h of exposure, there was a significant reduction of the peak absorbance of the stretching C–C of the aromatic bonds located close to 1509 cm^{-1} (Fig. S6(b)†). For unfilled epoxy and nano-filled composites (in Fig. 1(a) to (d)), peaks related to carbonyl (1700–1800 cm^{-1}) and hydroxyl groups (3600–3200 cm^{-1}) increased with degradation. This degradation was more extensive for additive-free epoxy. A decrease in the absorption peaks occurred in spectral regions that corresponded to absorbance by the N–H bond at 773 cm^{-1}, stretching of the C–O bond of the oxirane group at 915 cm^{-1}, and of the C–O–C bond of ethers at 1036 cm^{-1}, while peaks corresponding to aromatic ring C═C at 1608 cm^{-1} showed more persistence. Since the IR absorption peaks have been correlated with the epoxy chemical structure, a decrease in the absorption peak heights and areas can be associated with the photochemical reaction of the functional groups and a loss of products. With the increase in aging time decreases in absorbance were observed for the aromatic bond at 1606 cm^{-1}, the isopropylidene group at 1183 cm^{-1}, and the ether bond at 1028 cm^{-1} (Fig. S6(a)†). The next section discusses how chemical and physical changes accelerate the degradation of the epoxy surface by providing a path for water or contaminants to penetrate below the surface.

The oxidation of the epoxy resin results in the formation of carbonyl groups, shown in the ATR-FTIR spectra between 1670–1790 cm^{-1}. There was a small increase in absorbance in this region with aging, signifying degradation. The CI increased by a factor of four after 1000 h of aging for the unfilled epoxy, whereas for the nanofilled epoxy the increase was only 20 to 60%, depending on the type of filler [Fig. S5 and S6(a) in the ESI†]. The increase in the carbonyl peak lessened due to the addition of nano-carbon materials. After 2500 h of aging, the CI of epoxy, epoxy with CB, CNT and graphene were about 3, 1.29, 1.76 and 1.06, respectively. The inclusion of the nano-carbon fillers reduced the magnitude of the CI (compared to the pure epoxy), indicating they reduced the extent of polymer degradation in the top few microns of the sample.

A broad peak between 3600 cm^{-1} and 3000 cm^{-1}, corresponding to hydroxyl groups, increased due to photo- and chemical oxidation during aging.[58,59] At more pronounced aging conditions, changes in two broad peaks of the spectra centered at 3420 cm^{-1} and 2920 cm^{-1} were observed: these peaks correspond to an increase in the intensity of O–H stretching and decreased intensity of the C–H stretching, respectively.

3.2 Changes in surface morphology of composites induced by weathering

Changes in the physical, mechanical structural properties of polymers due to weathering are of significant concern when anticipating their longevity in applications, forming cracks due to the oxidation of the internal polymer matrix.[29,31,53,60–62] Thus, environmental stress cracking of polymers is a common cause of failure in polymers, including a loss of elasticity particularly for amorphous polymers such as epoxy.[31,54,60,63–67]

In this study, imaging was used to investigate crack formation on the surface of weathered epoxy, with and without nanofillers. The impacts of weathering on polypropylene (PP) were also investigated to determine the degree to which crack formation depended on the composite's matrix material. Photomicrographs (250×) comparing the surfaces of un-degraded and degraded polymers and composites are shown in Fig. 2. Fig. 2(A) to (E) show images of surfaces of unaged pristine epoxy and epoxy filled with nanomaterials. All aged epoxy samples exhibited obvious cracks but both polypropylene samples showed much less degradation [Fig. 2(F) and (G)].

A closer look at the aged surface analysis is provided by SEM imaging. Fig. 3 shows SEM images of unfilled epoxy and epoxy filled with either CB, graphene, MWCNT, or SiO_2 before aging (left column) and after aging (center column)

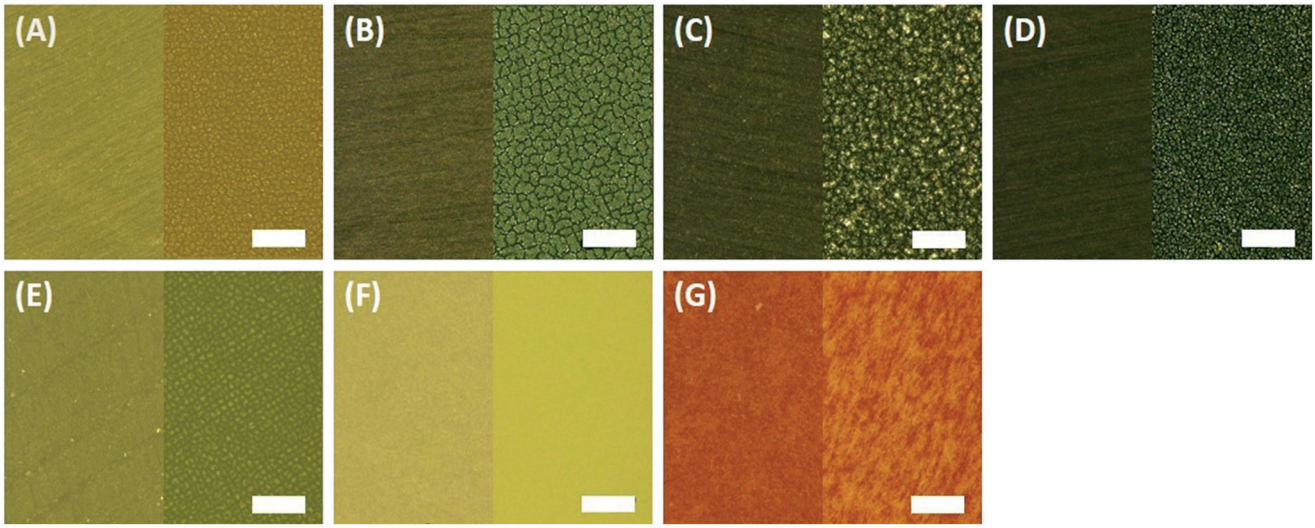

Fig. 2 Optical images (250×) of surfaces of: (A) unfilled epoxy, (B) epoxy–carbon black composite, (C) epoxy–graphene composite, (D) epoxy–MWCNT composite, (E) epoxy–SiO_2 composite, (F) unfilled polypropylene, (G) PP–Fe_2O_3. The left half of each image shows un-weathered sample and the right half shows samples weathered for 2500 h in an accelerated wet weathering chamber. Scale bar is 250 μm for all images.

for 2500 h. As seen by comparing the images in Fig. 3, the amounts of micro-cracks on the surface of the materials were much more significant after aging, leading to enhanced surface roughness. The type of filler did not have a visible influence on crack formation. Kumar *et al.* reported a similar structure of micro-cracks and matrix erosion in epoxy–carbon nanofiber nanocomposites by UV photooxidation and water condensation.[68]

All epoxy materials, including the pure matrix and the nanocomposites, behaved similarly. Cracking of the surface, oxidation of the epoxy matrix, and accumulation of ENM on the surface are observed for all materials, and in fact, resemble the surface of UV wet-aged polyurethane composite with the same type of ENM (CB, CNT, SiO_2).[35] SEM with energy dispersive X-ray (EDX) analysis was performed on a subset of samples available to EPA-Athens; see our previous paper for more detail related to this technique.[47] Specifically, SEM/EDX of epoxy–SiO_2 (1000 h aging) and polyamide–kaolin (2500 h aging) are highlighted in Fig. S9 of the ESI.† These two nanocomposites contain Si with significant abundance, which can be easily distinguished from the other polymer nanocomposites that we examined. The presence of kaolin is also confirmed with the detection of Al on the surface of the wafer. We assumed that similar particle-like formations were observed on the surface of all exposed samples and confirmation with EDX for these two samples is consistent with accumulation of ENM on the surface during the weathering process.

3.3 Changes in surface hydrophobicity of aged raw and aged epoxy composite

The impacts of nanofillers and environmental stress on wettability, adhesion properties, and repellence have many applications. Hydrophobic properties are useful for outdoor applications. The changes in the physical and chemical surface properties by weathering, the hydrophilicity, or wettability, of polymers' surface was observed by measuring static contact angles of aged samples at five selected points on the exposed surface.

The change in the contact angle for several epoxy materials with increased aging is shown in Fig. 4. There was little measurable difference in contact angles (81.6° ± 4.2) for most epoxy samples (nano-filled and unfilled), except for SiO_2-filled epoxy, which had a contact angle of 36.2° ± 1.0. This indicated that the hydrophilicity of the filler impacts the contact angle of composite materials. During aging, UV photooxidation and chemical oxidation started from the surface of the samples, and the more hydrophobic epoxy and nano-filled-epoxy stayed stable for the first 500 h. After 1000 h of accelerated aging, the contact angles for unfilled epoxy decreased to 31.4° ± 2.8, whereas epoxy filled with CNT, graphene and CB decreased to 42.5° ± 6.3°, 42.9° ± 14.5° and 76.6 ± 4.4°, respectively. After 2500 h, the average contact angles for graphene filled epoxy dropped to 22° ± 16°, whereas for CNT and CB filled epoxy the values were close to zero, indicating the materials became highly hydrophilic. SiO_2-Filled epoxy also grew more hydrophilic with increased aging, to the extent that it showed no measurable contact angle after 1000 h of weathering. The combination of changes in surface morphology, surface cracks and the release of filler materials could have resulted in the wettability of the test materials. This complete wetting was consistent with the accumulation of silica on the surface reported in earlier epoxy–SiO_2 aging studies.[45]

Contact angle and surface wettability depend on both the surface roughness and chemical functional groups. The previous two sections provide insight into how aging led to physical and chemical changes at the surface of the epoxy composites, which led to a significant decrease

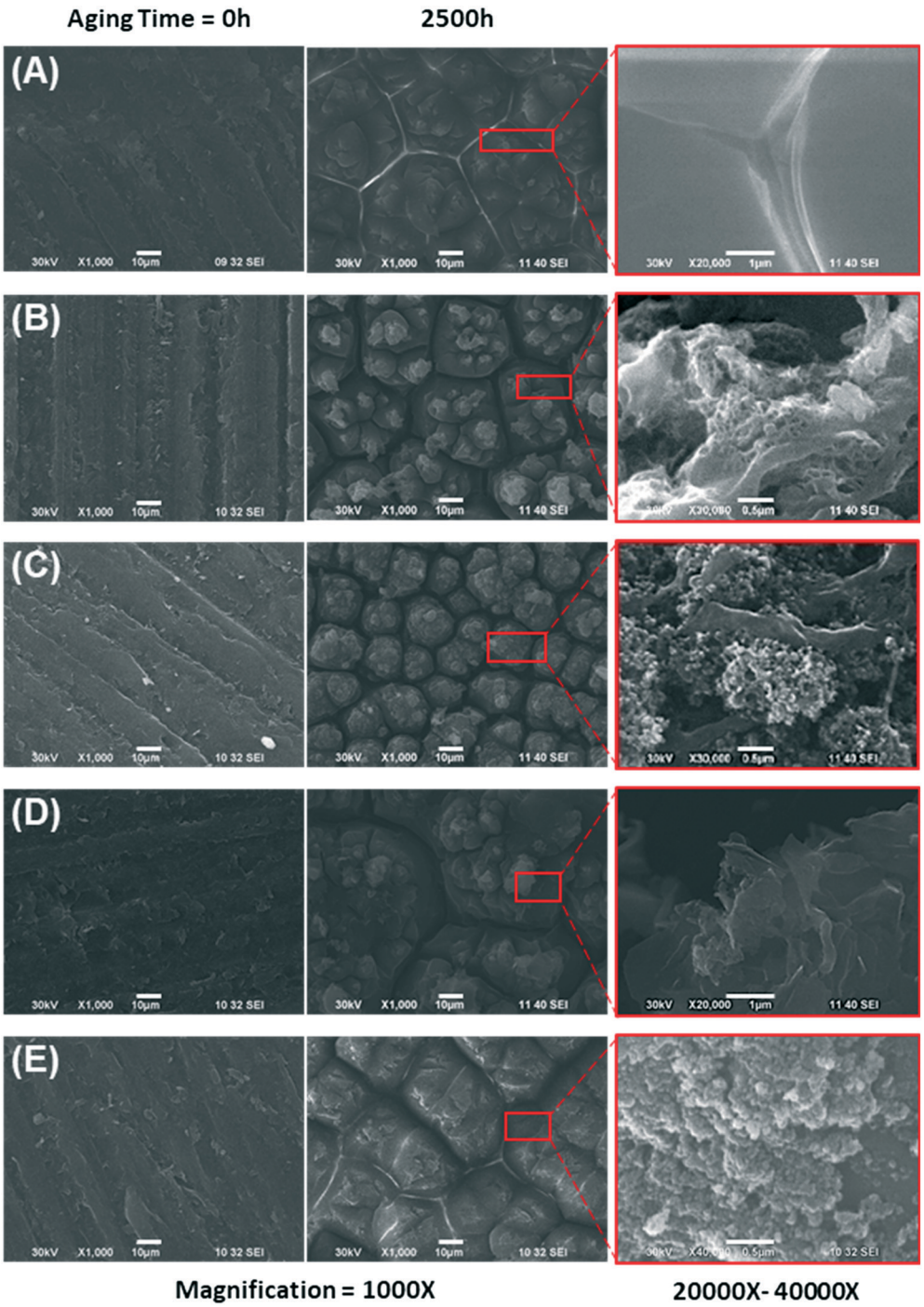

Fig. 3 Scanning electron microscope (1000×) images of the surface of un-degraded (0 h) and degraded (2500 h wet aging) samples (A) epoxy, (B) epoxy–MWCNT composite, (C) epoxy–carbon black composite, (D) epoxy–graphene composite, (E) epoxy–SiO_2 composite. The leftmost column shows un-degraded samples, the center column shows degraded samples, and the rightmost column shows insets of the center images with 20 000× to 40 000× magnification. Scale bar for the for two left column images are 10 μm, and for the right column image 0.5 μm.

in the measured contact angles. The increase in surface roughness with aging results in a reduction of the hydrophobicity.[69] The rise in wettability is also attributed to the formation of surface radicals and polar functional groups, such as carbonyls after polymer bonds broke.[54] These changes to the chemical structure at the surface were shown by the ATR-FTIR spectra in Fig. 1 and the accumulation of Si-containing ENMs on the surface shown by EDX analysis (Fig. S9†). Other studies reported UV-aged polymers became more hydrophilic due to the chemical modification of the surface by enrichment with structures containing carbonyl and hydroxyl bonds, and these changes lead to a monotonic improvement of hydrophilicity under UV irradiation.[63,70–72]

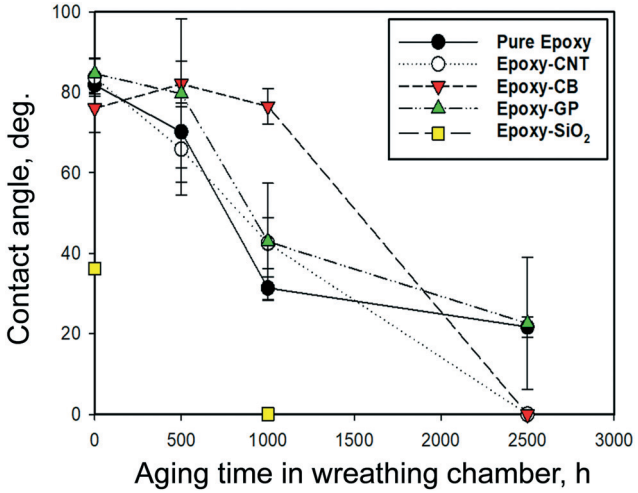

Fig. 4 Changes in the contact angle of unfilled and filled epoxy after selected amounts of weathering under wet conditions.

Our results indicate that the degradation of the polymer chains grows with an increase in the dose of UV irradiation of epoxy and nano-filled epoxy. Prolonged exposure resulted in the reaction between water molecules and reactive oxygen species with the epoxy molecular chain (which has a three-dimensional network structure). Wettability was shown to depend on aging time and the type of filler ENM in the epoxy. Increased wettability may result in increased water uptake that extends the deterioration of the polymer matrix away from the surface and into the bulk of the material. The effects of wet weathering on the loss of mass of wafers and thickness are shown in Fig. S7 and S8,† respectively.

3.4 Quantification of fragment release with options of fractionation and of dry or wet aging

The collection of leachate measurements is reported in Fig. 5. This graph displays the averaged absorption coefficients at 275 nm (α_{275}) of leaching water samples from epoxy (A) and PA (B) wafers with (wet) and without (dry) water spray in the aging chamber. As previously reported,[47] UV-vis spectroscopy can sensitively detect fragments or nanoparticles released from the wafers through changes in the absorbance (absorption and scattering by particles) of the suspension. As such, a higher α_{275} measured for the leaching water indicates a larger amount of material released.

As described in section 2.6, the α_{275} of leachate was analyzed with and without the fractionation step. Such a step was applied for the first time in the NanoRelease protocol with the aim to developing a more robust and consistent comparison system between the fractions of smaller particulates emitted from each material. In fact, the centrifugation step reduces the part of the sample larger than micro–nano dimension which can contribute disproportionately to the UV-vis signal by displaying high scattering. Considering samples with $\alpha_{275} > 0.05$, the

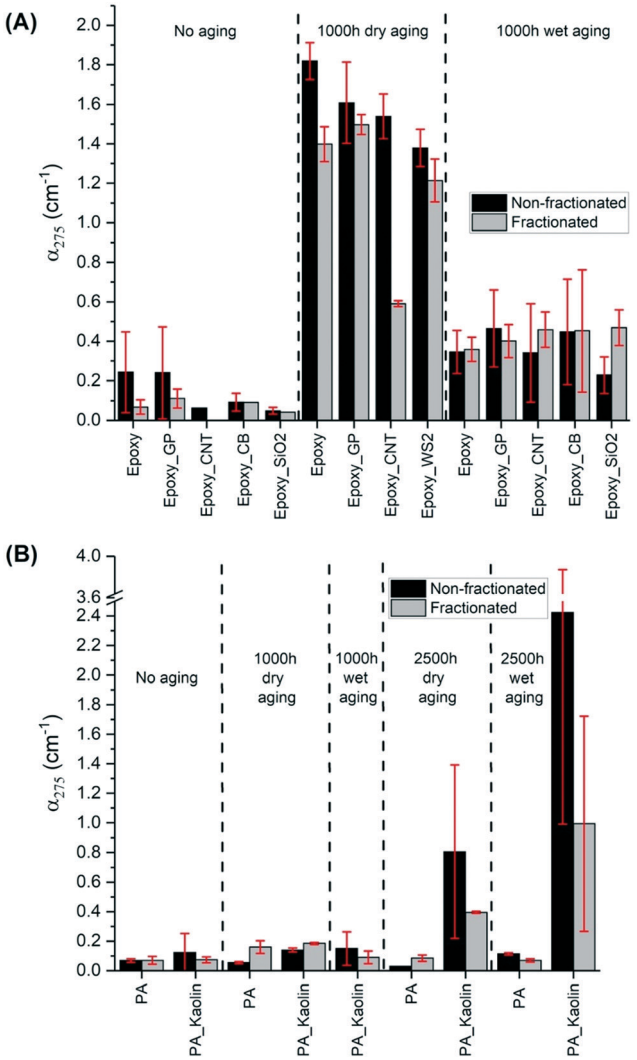

Fig. 5 Absorption coefficient measurements at 275 nm (α_{275}) of leaching fluids from (A) epoxy and (B) PA samples, resulting from different aging (time, wet/dry) and fractionation (fractionated/non-fractionated) protocols. Wet-aged samples were averaged between laboratories. Dry-aged samples were aged and analyzed by BASF only.

outcomes reveal that the centrifugation step effectively removed part of the sample reducing the magnitude of the absorption coefficient in most cases. Spectra of samples before and after fractionation are shown in Fig. S10 of the ESI.† For some wafers, the reduction is particularly large *e.g.* unaged pure epoxy, epoxy–CNT (dry-aged 1000 h) and PA–kaolin (aged 2500 h). For these three samples, either a high number of big fragments was present, or fragments were particularly large. For both cases, the fractionation effect was more pronounced. Interestingly, the reduction of the signal is often followed by a decrease of the error bar. The comparison between the relative standard deviation (RSD) of non-fractionated and fractionated samples, which are calculated in Table S1 in the ESI,† reveals that the fractionation step improves the reproducibility of the outcomes.

As expected, Fig. 5 shows that leachates of nearly all unaged wafers exhibited lower absorption coefficients than the aged ones. Although the wet aging protocol could have caused an amplified degradation due to matrix hydrolysis, and thus more release of polymer fragments and nanoforms, the experimental evidence (apart from PA–kaolin aged 2500 h) illustrates less fragment release compared to the dry-aged samples. One explanation could be that rain events in the chamber removed some of the debris from the wafer surface during weathering, reducing fragment concentration recovered in the leaching water. This somewhat clouds the interpretation of the results. Clearly more studies are needed to better understand the impact of leaching during the wet weathering. Dry weathering, an approach widely used by NIST,[14–16,37,45,46,73] appears to be preferable, at least for screening purposes, although not as environmentally relevant.

Notably, the UV-vis results of epoxy and PA NEP were compiled from three research centers (BASF and two USEPA). Comparing UV-vis measurements of released material between laboratories (Fig. S11 in the ESI†) generally shows good agreement compared to previous reports.[37] The variation remains under a factor of 3 in most cases before fractionation (data not shown) and remains under a factor 3 between two labs after fractionation. This finding supports earlier observations of quantitative agreement between laboratory analysis with UV-vis,[47] and extend the findings to composites with a variety of nanofillers. This demonstrates the ability to achieve reproducible results when following the experimental protocols for aging and analysis outlined in sections 2.3 and 2.6–8. Furthermore, this agreement between labs supports the combination of results from different analytical techniques housed at either BASF, EPA-CEMM, or EPA-CESER to provide a broader and more complete characterization of weathered surfaces and released material.

All the leaching water samples collected at BASF were also analyzed by AUC coupled with a refractive index detector (AUC-RI). Fig. S3 of the ESI† presents the concentration of the emitted particles from the different wafers. AUC provided also a direct measurement of the size distributions. The comparison of the turbidity before and after fractionation with a cut point of approximately 1 μm shows that for all materials approximately 80% of the fragments have a particle size below 1 μm. The AUC size distributions did not reveal characteristic size peaks of individual ENMs due to the extremely low ENM concentration in the leaching water samples. Such samples presented large liquid volume per irradiated specimen surface, even after applying a step of bubbling volume reduction.

The results in Fig. 5(A) and S3† show that the amount of release is mostly not influenced by the typology of the nanofiller apart from the CNT. The CNT-wafer displayed, in the dry condition, a significantly lower release compared to the others. The CNT addition in the epoxy matrix reduces the absorbance of the leachate by 42% compared to the pristine wafer. This is consistent with earlier observations of formation of a dense CNT network at the surface of aged CNT composites.[14] That network suppressed release after wet aging from relatively stable polymers such as polyamide, but increased release from a very photoreactive epoxy.[47] In the present study with a more resilient epoxy, after wet aging neither suppression nor increase of release by CNT was observed compared to the pristine wafer. The suppression was only observed after dry aging.

Silica has resulted in upmodulating the rate of aging in past studies,[74] but this effect was not observed here. Immersed sonication of the sprayed samples with SiO_2 filler exhibited interesting results compared to those with the carbon fillers. SiO_2 is much more UV-transparent than the carbon fillers and therefore the UV-exposure and thus photodegradation of the matrix in epoxy–SiO_2 composited samples is predicted to be greater. In agreement with this prediction and other previous results,[74] the fractionated leachate of samples of weathered epoxy–SiO_2 had slightly higher absorbance, though within error, than weathered epoxy alone.

As shown by previous studies and the results for epoxy in Fig. 5(A), matrix degradation is one significant pathway for the observed increases in leachate absorbance. For example in the study of Wohlleben *et al.*,[47] carbon nanomaterials are released by weathering of their epoxy matrix with the concurrent increase in absorbance of the leachate. In the study, the absorbance of the released CNT from epoxy wafers is correlated with the release of cobalt embedded in the CNT.[47] Except for CNT dry-aged epoxy wafers, our set of fractionated epoxy–carbon NM composites present slightly higher absorbances than epoxy itself. Although this higher release is within the error bar, it can be related to the emission of the carbon fillers, which contributed to increased absorbance with weathering of the epoxy samples. The observed UV-vis signal cannot be attributed directly to the pure nanomaterials, as the form of release (pure matrix, ENM protruding from or embedded in matrix, freely dispersed ENM) is only known after TEM identification.

Regarding PA composites (Fig. 5(B)), the other class of polymeric materials, the wafers were investigated with only a type of nanofiller, kaolin, at high concentration (25%). Considering the same aging conditions, fragment release from PA is notably less strong than from epoxy. Indeed, the average absorbance is only 0.1 for both unaged and 1000 h aged. PA wafers were subjected to a longer period of artificial aging (2500 h) to stress this material. In this case, the emission of debris is more evident for the wafers containing the nanofiller. The high concentration of the nanofillers enhanced the emission of fragments especially with wet treatment. However, the employment of a single filler is insufficient to confirm a different PA trend than observed with epoxy. Finally, PP wafers were also analyzed after a long aging period (2500 h). The results after the NanoRelease protocol displayed a very low emission of particles with an average absorbance of 0.1 for both filled and unfilled specimens. The related UV-vis spectra data were not reported

in this publication. These outcomes show how strong is the influence of the matrix properties embedding the nanofiller.

3.5 Ranking of fragment release against other NEPs

The rates of release from epoxy NEPs can be converted to a mass release rate in the range of 0.95 ± 0.71 mg MJ^{-1} (from AUC-RI) and an absorption coefficient rate of 3.7 ± 2.4 × 10^{-4} MJ^{-1} m^2 (from UV-vis). This metric corrects for all sampling-related parameters such as specimen area, immersion volume, bubbling reduction (more information is reported in the ESI†).

Additionally, the different contribution of dry and wet protocols to the total fragment emission can be also highlighted. In case of dry treatment, epoxy NEPs showed a mass release rate in the range of 0.83 ± 0.59 mg MJ^{-1} and an absorption coefficient rate of 6.0 ± 1.7 × 10^{-4} MJ^{-1} m^2. On the other hand, after wet aging epoxy NEPs mass release rate was 1.2 ± 0.9 mg MJ^{-1} and the absorption coefficient rate was 1.9 ± 0.4 × 10^{-4} MJ^{-1} m^2. On another set of epoxies with different polymer chemistry (bisphenol-A resin with dicyandiamide hardener), but with the same type of MWCNT, values of mass release of 5 mg MJ^{-1} and absorption coefficient rate of 3.1 × 10^{-3} MJ^{-1} m^2 were determined.[47] Similar values were observed for other epoxies.[74]

In comparison, the absorption coefficient rates from PP and PA NEPs are on the order of 2.6 × 10^{-5} MJ^{-1} m^2 and 9.8 10^{-5} MJ^{-1} m^2 respectively. The ranking of release rates epoxy

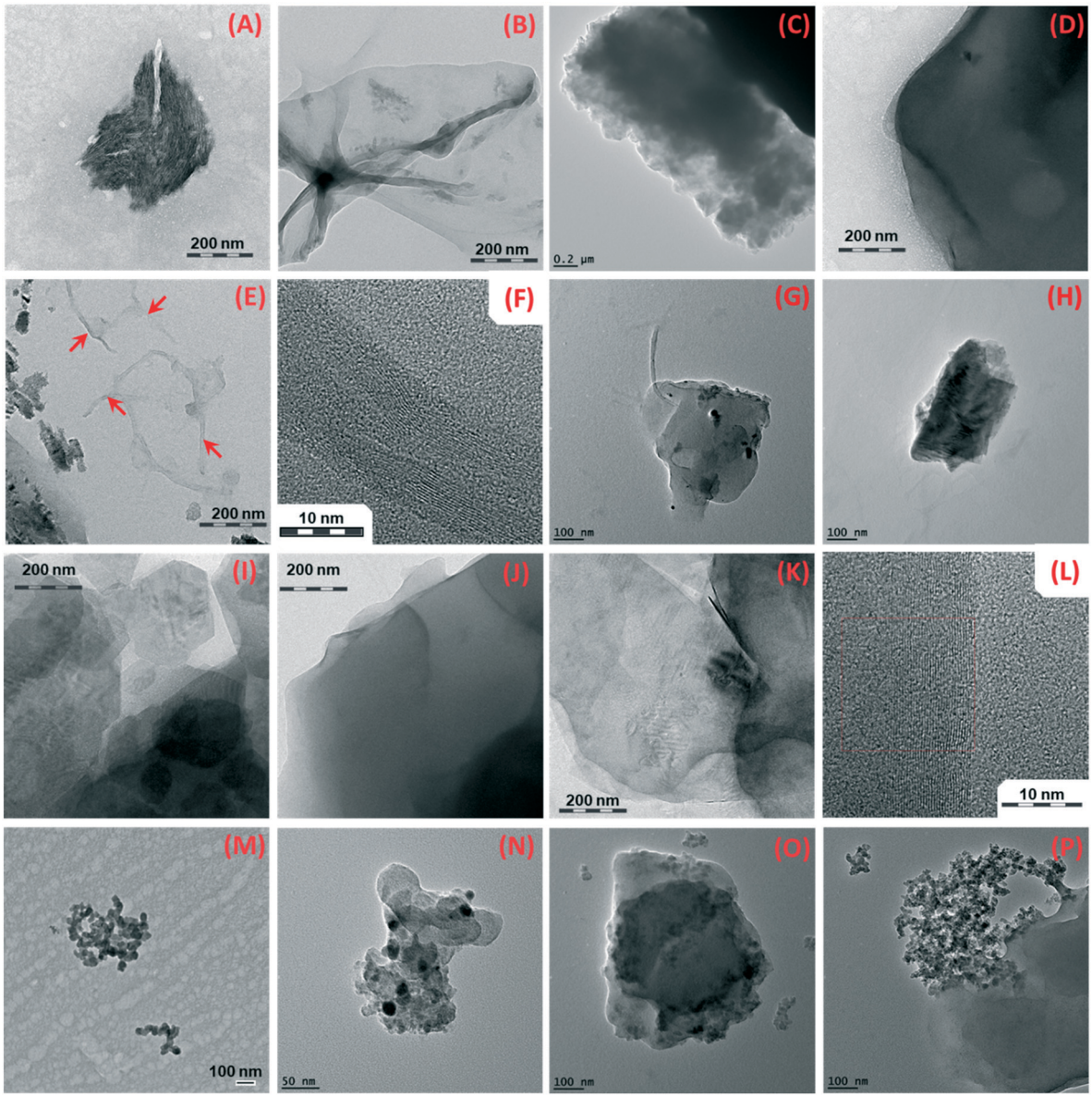

Fig. 6 Transmission electron microscope images of released polymer fragments and nanofillers from 1000 h aged wafers of unfilled epoxy under dry (A and B) and wet (C and D) conditions, epoxy–CNT under dry (E and F) and wet (G and H) conditions, epoxy–graphene under dry (I and J) and wet (K and L) conditions, epoxy–CB under wet (M and N) conditions and epoxy–SiO_2 under wet (O and P) conditions.

> PA > PP confirms the working hypothesis that the resilience of the polymer matrix is vital in limiting aging of the composites and nano-releases. Our results in Fig. 5 confirm that the primary importance of the polymer matrix still holds true for highly filled polymers, such as the PA with 25% kaolin, and few% of CB. An up-modulation of the PA release by kaolin is detectable, and can be assigned to the low UV absorption, low entanglement of the relatively stiff kaolin platelets. Interestingly, an earlier study found significant release induced by wet aging and direct sampling on PA–silica composite, assigned to hydrolysis.[17] Our PA does not show such effects, because the CB is added exactly for making the PA matrix more hydrophobic and thus resilient against the infiltration of water and ensuing hydrolysis. This is an essential performance characteristic for its intended use to replace metal parts by lower-weight polymer in automotive applications.

3.6 Imaging of released fragments

All the leaching liquids that originated from aged epoxy and PA specimens (except for WS_2 wafer) were analyzed by TEM. The drop samples were collected from the immersion fluids after sonication and bubbling, but before adding SDS. The surfactant can create salts on the grid, obscuring nanoforms in the images. Fig. 6 shows representative TEM images of leaching liquids of wafers weathered 1000 hours with dry and wet protocols. The first row presents fragments originated from epoxy wafers without nanofillers. Both protocols (wet and dry) resulted in release of polymer debris that often exceeded the nanoscale. In contrast, nanoforms were easily recognized in case of CNT–epoxy composites (in the second row). The CNT were released both as free nanoforms and as protruding CNT of particulate epoxy fragments. Fig. 6(E) shows the internal multi wall structure of nanotubes. In the third row, TEM pictures illustrates planar graphene sheets released again with both treatments. Selected area electron diffraction (SAED) technique was employed to support TEM observations. SAED analysis reveals the characteristic hexagonal diffraction pattern of graphene structure (Fig. S13†) confirming TEM determination.[75] More details are given in the related ESI† section. In the last row, both CB and SiO_2 nanoforms were successfully detected by TEM either as free forms or as protrusions from larger fragments. The NanoRelease protocol produces both free and embedded ENM release for all specimen series. Additional TEM images are included in the ESI† of particles released from neat epoxy (Fig. S14†), epoxy–CNT (Fig. S15†), and epoxy–GP (Fig. S16†) after both wet and dry aging protocols.

The release from PA wafers was also evaluated by TEM (Fig. 7). As for epoxy nanocomposites, fragments of polymer and of nanofiller (kaolin, Fig. 7G) were detected in the immersion water after applying the NanoRelease protocol.

Sufficient number of TEM scans were not collected in this study for any statistically relevant differentiation of the form of release as done earlier in the NanoRelease inter-lab comparison,[47] but we can conclude that matrix/ENM fragments prevail and occasionally individual ENMs are observed for all materials. The ultramicrotomy analysis shows that our NEPs are rather well dispersed and compatibilized with the polymer matrix, such that modulation by compatibilization, as inferred to interpret differences between different PA composites,[18] probably do not apply here.

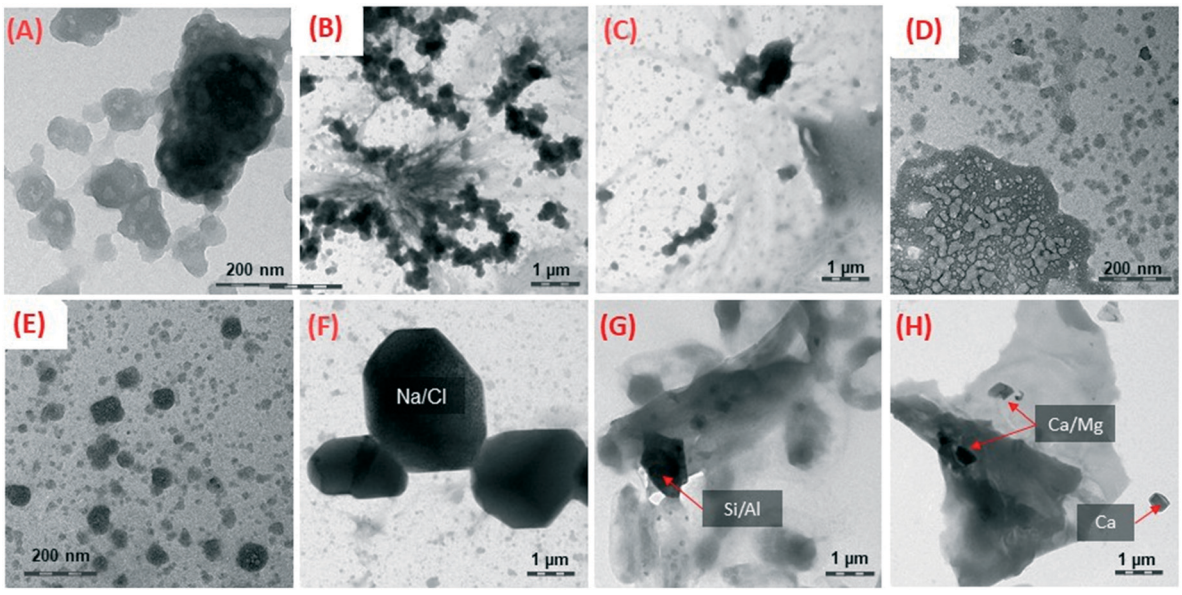

Fig. 7 A selection of TEM pictures of debris present in the leachates of PA wafers. In the first row, PA wafers were aged (A and B) 0 h and (C and D) 2500 h in the second row, PA–kaolin wafers were weathered (E and F) 0 h and (G and H) 1000 h.

3.7 Chemical characterization of embedded nanomaterials

Raman spectroscopy enables further characterization of structural, electronic, and vibrational properties of materials. We used this technique to study released fragments from three of our epoxy composites containing carbonaceous nanomaterials. The Raman spectra of these fragments (found in Fig. S17 in the ESI†) were compared to those of their corresponding pure nanofillers to evaluate the influence of weathering on the ENM chemical structure. Utilization of a 785 nm excitation wavelength enabled us to resolve both the disorder induced D-band (~1320 cm^{-1}) and G-band (~1600 cm^{-1}), with the G-band corresponding to the crystalline-graphitic and in-plane vibrations of sp^2 hybridized carbon. The ratio of the intensity of the D and G bands (I_D/I_G) indicates the relative amount of disorder present in the sample.[76,77] Disorder was higher in both epoxy–MWCNT (1.68 compared to 1.55) and epoxy–GP (1.08 compared to 0.56) weathered leachates relative to their respective pure ENMs. This was expected due to the fact that the weathering process has been shown by prior studies to increase functionalization along MWCNT chains.[76] Interestingly, despite MWCNT having a much larger I_D/I_G ratio (more disorder) than graphene ENMs,[77] graphene is much more[14,78,79] easily transformed upon weathering, as shown with the approximate doubling of the I_D/I_G ratio. This is likely due to the creation of defects in graphene.[80–82] These results coupled with TEM-SAED analysis offer a qualitative assessment of release and detection, and yield insight into the localized hybridization of carbon upon weathering.

4. Conclusions and next steps

We amended the previously validated NanoRelease protocol[47] by adding optional fractionation, enhancing the ability of future users to assess the content of submicron fragments released by weathering using widespread techniques, such as tabletop centrifugation and UV-vis spectroscopy. In leachates from our range of epoxy, PA, and PP nanocomposites, we found a dominance of sub-micron fragments that were consistent with TEM and AUC analyses. The results were robust between three independent laboratories. We also expanded the scope of our weathering experiments by comparing wet and dry aging[14,78,79] and by studying the kinetics of aging. Though not as environmentally relevant, dry weathering provides better control of released particles than wet, making it preferable when comparing release from different materials. Quantitative studies can now use the enhanced protocol to follow up on the modulation of weathering by wavelength[83–85] and by molecularly dissolved additives (UV-stabilizers, pro-oxidants).

Among a systematic series of ENM fillers (MWCNT, WS_2, SiO_2, carbon black, graphene) that are black or UV transparent, stiff or entangled, the particles of fiber or platelet, MWCNTs were unique in forming a densely entangled network on the aging polymer surface that tended to reduce release by UV-absorption and mechanical stabilisation.[14] We found a ranking of degradation and release in the order of epoxy > PA > PP, with modulation by the embedded ENM. In a real-world automotive PA with multiple fillers at total >35% filler content, the matrix remains the most important parameter, with a slight increase of release by kaolin platelets, but a significant reduction of hydrolytic aging and release by the hydrophobic CB.

The similarity between the different nanomaterials, with respect to a potential hazard, exposure, and risk, is key to grouping frameworks.[12,86,87] Here, we showed how comparative testing of the lifecycle releases from NEPs by the NanoRelease protocol[47] could support the hypothesis that polymer matrix is more important than actual ENM for predicting the rate and form and, ultimately, risk of released fragments under intended use and stress (*e.g.*, outdoor use, with weathering stresses). Considering all the evidence, these results support "grouping by lifecycle" for the family of epoxy NEPs in estimating environmental exposure during the use phase. Therefore, future NEPs will not need to be assessed case-by-case; instead, environmental risk estimates can be read from one NEP to another that shares the same matrix and same intended use. Our approach supports independent findings that the hazard potential was highly similar for fragments from epoxy with or without embedded CNTs,[15,88,89] and this extended to other NEPs of the same matrix but different (or no) ENM, for humans[27,89–93] and the environment.[23] A standard is being developed in ISO TC229 to enable decision-making in a stepwise approach that starts with the intended use, then matrix, ENM, and current grouping frameworks by the GRACIOUS or nanoGRAVUR[94] framework that incorporates lifecycle releases by the same logic. Consideration of lifecycle remains important because weathering induces slow releases but occasionally releases free ENM and is thus a pathway of environmental emission.

Conflicts of interest

ER, KV, WW are employees of BASF SE, a company producing and marketing nanomaterials.

Acknowledgements

This polymer weathering inter-comparison and collaboration would not have been possible without the fabrication of test specimen at University of Kaiserslautern, and the dedicated laboratory support of Thorsten Wieczorek and Philipp Mueller. This work was partially funded by the BMBF (German Federal Ministry of Education and Research) project nanoGRAVUR – Nanostructured materials – Grouping in view of worker, consumer and environmental safety and risk minimization (FKZ 03XP0002X). This research was performed while MJBD and HSH held NRC research associateship awards at U.S. EPA. This project was supported in part by an appointment to the Research Participation Program at both ORD/CEMM and ORD/CESER, U.S. Environmental Protection Agency, administered by the Oak Ridge Institute for Science

and Education (ORISE) through an interagency agreement between the U.S. Department of Energy and EPA. The views expressed in this article are those of the authors and do not necessarily represent the views or policies of the U.S. Environmental Protection Agency.

References

1 W. Wohlleben, C. Punckt, J. Aghassi-Hagmann, F. Siebers, F. Menzel, D. Esken, C.-P. Drexel, H. Zoz, H. U. Benz, A. Weier, M. Hitzler, A. I. Schäfer, L. D. Cola and E. A. Prasetyanto, Nanoenabled Products: Categories, Manufacture, and Applications: Protocols and Industrial Innovations, in *Metrology and Standardization for Nanotechnology: Protocols and Industrial Innovations*, ed. E. Mansfield, D. L. Kaiser, D. Fujita and M. Van de Voorde, John Wiley & Sons, 2017, pp. 411–464.

2 Ministère de l'Environnement and de l'Énergie et de la Mer, *Éléments issus des déclarations des substances à l'état nanoparticulaire: Exercice 2015*, 2015.

3 EPA, Final Rule: Chemical Substances When Manufactured or Processed as Nanoscale Materials, in *TSCA Reporting and Recordkeeping Requirements*, 2017, vol. 82.

4 H. Wigger, W. Wohlleben and B. Nowack, Redefining environmental nanomaterial flows: Consequences of the regulatory nanomaterial definition on the results of environmental exposure models, *Environ. Sci.: Nano*, 2018, **5**, 1372–1385.

5 A. Caballero-Guzman and B. Nowack, A critical review of engineered nanomaterial release data: Are current data useful for material flow modeling?, *Environ. Pollut.*, 2016, **213**, 502–517.

6 T. Sun, D. M. Mitrano, N. A. Bornhöft, M. Scheringer, K. Hungerbuehler and B. Nowack, Envisioning nano release dynamics in a changing world: using dynamic probabilistic modelling to assess future environmental emissions of engineered nanoparticles, *Environ. Sci. Technol.*, 2017, **51**(5), 2854–2863.

7 J. J. Scott-Fordsmand, J. M. Navas, K. Hund-Rinke, B. Nowack and M. J. B. Amorim, Nanomaterials to microplastics: Swings and roundabouts, *Nano Today*, 2017, **17**, 7–10.

8 C. Kingston, R. Zepp, A. Andrady, D. Boverhof, R. Fehir, D. Hawkins, J. Roberts, P. Sayre, B. Shelton, Y. Sultan, V. Vejins and W. Wohlleben, Release Characteristics of Selected Carbon Nanotube Polymer Composites, *Carbon*, 2014, **68**, 33–57.

9 Y. Lv, Y. Huang, J. Yang, M. Kong, H. Yang, J. Zhao and G. Li, Outdoor and accelerated laboratory weathering of polypropylene: A comparison and correlation study, *Polym. Degrad. Stab.*, 2015, **112**, 145–159.

10 T. van Harmelen, E. K. Zondervan-van den Beuken, D. H. Brouwer, E. Kuijpers, W. Fransman, H. B. Buist, T. N. Ligthart, I. Hincapié, R. Hischier, J. Studer, L. Hilty, C. Som and B. Nowack, LICARA nanoSCAN-A tool for the self-assessment of benefits and risks of nanoproducts, *Environ. Int.*, 2016, **91**, 150–160.

11 S. F. Hansen, K. A. Jensen and A. Baun, NanoRiskCat: a conceptual tool for categorization and communication of exposure potentials and hazards of nanomaterials in consumer products, *J. Nanopart. Res.*, 2014, **16**(1), 2195.

12 Z. A. Collier, A. J. Kennedy, A. R. Poda, M. F. Cuddy, R. D. Moser, R. I. MacCuspie, A. Harmon, K. Plourde, C. D. Haines and J. A. Steevens, Tiered guidance for risk-informed environmental health and safety testing of nanotechnologies, *J. Nanopart. Res.*, 2015, **17**(3), 155.

13 G. Pfaff, *Inorganic Pigments*, De Gruyter, Berlin, 2017, p. 329.

14 T. Nguyen, E. J. Petersen, B. Pellegrin, J. M. Gorham, T. Lam, M. Zhao and L. Sung, Impact of UV irradiation on multiwall carbon nanotubes in nanocomposites: Formation of entangled surface layer and mechanisms of release resistance, *Carbon*, 2017, **116**, 191–200.

15 J. Ging, R. Tejerina-Anton, G. Ramakrishnan, M. Nielsen, K. Murphy, J. M. Gorham, T. Nguyen and A. Orlov, Development of a conceptual framework for evaluation of nanomaterials release from nanocomposites: Environmental and toxicological implications, *Sci. Total Environ.*, 2014, **473**, 9–19.

16 E. J. Petersen, T. Lam, J. M. Gorham, K. C. Scott, C. J. Long, D. Stanley, R. Sharma, J. Alexander Liddle, B. Pellegrin and T. Nguyen, Methods to Assess the Impact of UV Irradiation on the Surface Chemistry and Structure of Multiwall Carbon Nanotube Epoxy Nanocomposites, *Carbon*, 2014, **69**, 194–205.

17 W. Wohlleben, G. Vilar, E. Fernández-Rosas, D. González-Gálvez, C. Gabriel, S. Hirth, T. Frechen, D. Stanley, J. Gorham, L.-P. Sung, H.-C. Hsueh, Y.-F. Chuang, T. Nguyen and S. Vazquez-Campos, A pilot interlaboratory comparison of protocols that simulate aging of nanocomposites and detect released fragments, *Environ. Chem.*, 2014, **11**(4), 402–418.

18 E. Fernández-Rosas, G. Vilar, G. Janer, D. González-Gálvez, V. Puntes, V. Jamier, L. Aubouy and S. Vázquez-Campos, Influence of Nanomaterial Compatibilization Strategies on Polyamide Nanocomposites Properties and Nanomaterial Release during the Use Phase, *Environ. Sci. Technol.*, 2016, **50**(5), 2584–2594.

19 M. Busquets-Fite, E. Fernandez, G. Janer, G. Vilar, S. Vazquez-Campos, R. Zanasca, C. Citterio, L. Mercante and V. Puntes, Exploring release and recovery of nanomaterials from commercial polymeric nanocomposites, *J. Phys.: Conf. Ser.*, 2013, **429**(1), 012048.

20 G. Vilar, E. Fernandez-Rosas, V. Puntes, V. Jamier, L. Aubouy and S. Vazquez-Campos, Monitoring migration and transformation of nanomaterials in polymeric composites during accelerated aging, *J. Phys.: Conf. Ser.*, 2013, **429**(1), 012044.

21 L. Schlagenhauf, B. Kianfar, T. Buerki-Thurnherr, Y.-Y. Kuo, A. Wichser, F. Nuesch, P. Wick and J. Wang, Weathering of a carbon nanotube/epoxy nanocomposite under UV light and in water bath: impact on abraded particles, *Nanoscale*, 2015, **7**(44), 18524–18536.

22 S. Harper, W. Wohlleben, M. Doa, B. Nowack, S. Clancy, R. Canady and A. Maynard, Measuring Nanomaterial Release from Carbon Nanotube Composites: Review of the State of the Science, *J. Phys.: Conf. Ser.*, 2015, **617**(1), 012026.

23 M. J. B. Amorim, S. Lin, K. Schlich, J. M. Navas, A. Brunelli, N. Neubauer, K. Vilsmeier, A. L. Costa, A. Gondikas, T. Xia, L. Galbis, E. Badetti, A. Marcomini, D. Hristozov, F. V. D. Kammer, K. Hund-Rinke, J. J. Scott-Fordsmand, A. Nel and W. Wohlleben, Environmental Impacts by Fragments Released from Nanoenabled Products: A Multiassay, Multimaterial Exploration by the SUN Approach, *Environ. Sci. Technol.*, 2018, **52**, 1514–1524.

24 N. Neubauer, W. Wohlleben and Ž. Tomović, Conductive plastics: comparing alternative nanotechnologies by performance and life cycle release probability, *J. Nanopart. Res.*, 2017, **19**(3), 112.

25 Y. Ding, W. Wohlleben, M. Boland, K. Vilsmeier and M. Riediker, Nano-object Release During Machining of Polymer-Based Nanocomposites Depends on Process Factors and the Type of Nanofiller, *Ann. Work Exposures Health*, 2017, wxx081.

26 S. Hirth, L. G. Cena, G. Cox, Z. Tomovic, T. M. Peters and W. Wohlleben, Scenarios and methods that induce protruding or released CNTs after degradation of composite materials, *J. Nanopart. Res.*, 2013, **15**, 1504.

27 W. Wohlleben, M. W. Meier, S. Vogel, R. Landsiedel, G. Cox, S. Hirth and Ž. Tomović, Elastic CNT–polyurethane nanocomposite: synthesis, performance and assessment of fragments released during use, *Nanoscale*, 2013, **5**(1), 369–380.

28 C. Han, E. Sahle-Demessie, A. Q. Zhao, T. I. Richardson and J. Wang, Environmental aging and degradation of multiwalled carbon nanotube reinforced polypropylene, *Carbon*, 2018, **129**, 137–151.

29 A. L. Andrady, H. Hamid and A. Torikai, Effects of solar UV and climate change on materials, *Photochem. Photobiol. Sci.*, 2011, **10**(2), 292–300.

30 B. Avant, D. Bouchard, X. Chang, H.-S. Hsieh, B. Acrey, Y. Han, J. Spear, R. Zepp and C. D. Knightes, Environmental fate of multiwalled carbon nanotubes and graphene oxide across different aquatic ecosystems, *NanoImpact*, 2019, **13**, 1–12.

31 D. Feldman, Polymer weathering: Photo-oxidation, *J. Polym. Environ.*, 2002, **10**(4), 163–173.

32 I. Fenoglio, M. Tomatis, D. Lison, J. Muller, A. Fonseca, J. B. Nagy and B. Fubini, Reactivity of carbon nanotubes: free radical generation or scavenging activity?, *Free Radical Biol. Med.*, 2006, **40**, 1227–1233.

33 M. Martinez-Morlanes, P. Castell, P. J. Alonso, M. T. Martinez and J. J. C. Puertolas, Multi-walled carbon nanotubes acting as free radical scavengers in gamma-irradiated ultrahigh molecular weight polystyrene composites, *Carbon*, 2012, **50**(7), 2442–2452.

34 S. Singh, Y. Pei, R. Miller and P. Sundararajan, Long-range, entangled carbon nanotube networks in polycarbonate, *Adv. Funct. Mater.*, 2003, **13**(11), 868–872.

35 W. Wohlleben, J. Meyer, J. Muller, P. Muller, K. Vilsmeier, B. Stahlmecke and T. A. J. Kuhlbusch, Release from nanomaterials during their use phase: combined mechanical and chemical stresses applied to simple and multi-filler nanocomposites mimicking wear of nano-reinforced tires, *Environ. Sci.: Nano*, 2016, **3**, 1036–1051.

36 Y. Ding, W. Wohlleben, M. Boland, K. Vilsmeier and M. Riediker, Nano-object Release During Machining of Polymer-Based Nanocomposites Depends on Process Factors and the Type of Nanofiller, *Ann. Work Exposures Health*, 2017, **61**(9), 1132–1144.

37 D. S. Jacobs, S.-R. Huang, Y.-L. Cheng, S. A. Rabb, J. M. Gorham, P. J. Krommenhoek, L. L. Yu, T. Nguyen and L. Sung, Surface degradation and nanoparticle release of a commercial nanosilica/polyurethane coating under UV exposure, *J. Coat. Technol. Res.*, 2016, **13**(5), 735–751.

38 J. M. Gorham, T. Nguyen, C. Bernard, D. Stanley and R. David Holbrook, Photo-induced surface transformations of silica nanocomposites, *Surf. Interface Anal.*, 2012, **44**(13), 1572–1581.

39 J. Markarian, Automotive and packaging offer growth opportunities for nanocomposites, *Plast. Addit. Compd.*, 2005, **7**(6), 18–21.

40 K. Müller, E. Bugnicourt, M. Latorre, M. Jorda, Y. Echegoyen Sanz, J. M. Lagaron, O. Miesbauer, A. Bianchin, S. Hankin and U. Bölz, Review on the processing and properties of polymer nanocomposites and nanocoatings and their applications in the packaging, automotive and solar energy fields, *Nanomaterials*, 2017, **7**(4), 74.

41 C. Bernard, T. L. Nguyen, B. Pellegrin, R. D. Holbrook, M. Zhao and J. Chin, Fate of graphene in polymer nanocomposite exposed to UV radiation, *J. Phys.: Conf. Ser.*, 2011, **304**(1), 012063.

42 D. González-Gálvez, G. Janer, G. Vilar, A. Vílchez and S. Vázquez-Campos, The Life Cycle of Engineered Nanoparticles, in *Modelling the Toxicity of Nanoparticles*, ed. L. Tran, M. A. Bañares and R. Rallo, Springer International Publishing, Cham, 2017, pp. 41–69.

43 E. Zohar, S. Baruch, M. Shneider, H. Dodiuk, S. Kenig, R. Tenne and H. D. Wagner, The Effect of WS2 Nanotubes on the Properties of Epoxy-Based Nanocomposites, *J. Adhes. Sci. Technol.*, 2011, **25**(13), 1603–1617.

44 P. C. Raynor, J. I. Cebula, J. S. Spangenberger, B. A. Olson, J. M. Dasch and J. B. D'Arcy, Assessing Potential Nanoparticle Release During Nanocomposite Shredding Using Direct-Reading Instruments, *J. Occup. Environ. Hyg.*, 2012, **9**(1), 1–13.

45 H.-C. Hsueh, D. S. Jacobs, J. M. Gorham, S. A. Rabb, L. L. Yu, C.-C. Tien, T. Nguyen and L. Sung, Kinetics of photodegradation and nanoparticle surface accumulation of a nanosilica/epoxy coating exposed to UV light, *J. Coat. Technol. Res.*, 2017, 1–10.

46 L. Sung, D. Stanley, J. M. Gorham, S. Rabb, X. Gu, L. L. Yu and T. Nguyen, A quantitative study of nanoparticle release from nanocoatings exposed to UV radiation, *J. Coat. Technol. Res.*, 2015, **12**, 121–135.

47 W. Wohlleben, C. Kingston, J. Carter, E. Sahle-Demessie, S. Vázquez-Campos, B. Acrey, C.-Y. Chen, E. Walton, H. Egenolf, P. Müller and R. Zepp, NanoRelease: Pilot interlaboratory comparison of a weathering protocol applied to resilient and labile polymers with and without embedded carbon nanotubes, *Carbon*, 2017, **113**, 346–360.

48 C. Andersson, *Composite laminates: Properties, performance and applications*, Nova Science Publishers, New York, 2010.

49 M. U. Amin and G. Scott, Photo-initiated oxidation of polyethylene effect of photo-sensitizers, *Eur. Polym. J.*, 1974, **10**(11), 1019–1028.

50 Y. Xing, L. S. Li, C. C. Chusei and R. V. Hull, Sonochemical oxidation of multiwalled carbon nanotubes, *Langmuir*, 2005, **21**(9), 4185–4190.

51 M. R. Hoffmann, I. Hua and R. Höchemer, Application of ultrasonic irradiation for the degradation of chemical contaminants in water, *Ultrason. Sonochem.*, 1996, **3**(3), S163–S172.

52 S. Uran, A. Alhani and C. Silva, Study of ultraviolet-visible light absorbance of exfoliated graphite forms, *AIP Adv.*, 2017, **7**(3), 035323.

53 L. Audouin, V. Langlois, J. Verdu and J. C. M. de Bruijn, Role of oxygen diffusion in polymer ageing: kinetic and mechanical aspects, *J. Mater. Sci.*, 1994, **29**(3), 569–583.

54 M. C. Celina, A. R. Dayile and A. Quintana, A perspective on the inherent oxidation sensitivity of epoxy materials, *Polymer*, 2013, **54**(13), 3290–3296.

55 N. J. H. Al-Mashhadan and S. Mohamad, Study of Degradation Effect on Physical Properties of Methyl Orange Doped PMMA, *J. Eng. Technol.*, 2011, **29**(1), 20–32.

56 T. Çaykara and O. Güven, UV degradation of poly(methyl methacrylate) and its vinyltriethoxysilane containing copolymers, *Polym. Degrad. Stab.*, 1999, **65**(2), 225–229.

57 M. A. Salih, B. M. Ahmad, A. N. Ibrahim, Z. K. Dahlan, R. Tajau, H. M. Mahmood and M. W. Yunus, Synthesis of Radiation Curable Palm Oil–Based Epoxy Acrylate: NMR and FTIR Spectroscopic Investigations, *Molecules*, 2015, **20**(8), 14191–14211.

58 V. Mylläri, T.-P. Ruoko and S. Syrjälä, A comparison of rheology and FTIR in the study of polypropylene and polystyrene photodegradation, *J. Appl. Polym. Sci.*, 2015, **132**(28), 42246–42263.

59 L. Barbes, C. Radulescu and C. Stihi, ATR-FTIR spectrometry characterisation of polymeric materials, *Rom. Rep. Phys.*, 2014, **66**(3), 765–777.

60 J. C. Arnold, Environmental stress crack initiation in glassy polymers, *Trends Polym. Sci.*, 1996, **4**(12), 403–408.

61 F. Awaja, S. Zhang, M. Tripathi, A. Nikiforov and N. Pugno, Cracks, microcracks and fracture in polymer structures: Formation, detection, autonomic repair, *Prog. Mater. Sci.*, 2016, **83**, 536–573.

62 M. Chowdhury, X. Sheng, F. Ziebert, A. C. M. Yang, A. Sepe, U. Steiner and G. Reiter, Intrinsic Stresses in Thin Glassy Polymer Films Revealed by Crack Formation, *Macromolecules*, 2016, **49**(23), 9060–9067.

63 A. S. Maxwell, W. R. Broughton, G. D. Dean and G. D. Sims, Review of accelerated ageing methods and lifetime prediction techniques for polymeric materials, *National Physical Laboratory-NPL Report DEPC MPR 016*, 2005, vol. PDB: 391516, p. 22.

64 B. Fayolle, L. Audouin and J. Verdu, Oxidation induced embrittlement in polypropylene — a tensile testing study, *Polym. Degrad. Stab.*, 2000, **70**(3), 333–340.

65 S. Girois, P. Delprat, L. Audouin and J. Verdu, Oxidation thickness profiles during photooxidation of non-photostabilized polypropylene, *Polym. Degrad. Stab.*, 1997, **56**(2), 169–177.

66 B. Fayolle, L. Audouin and J. Verdu, A critical molar mass separating the ductile and brittle regimes as revealed by thermal oxidation in polypropylene, *Polymer*, 2004, **45**(12), 4323–4330.

67 B. Fayolle, X. Colin, L. Audouin and J. Verdu, Mechanism of degradation induced embrittlement in polyethylene, *Polym. Degrad. Stab.*, 2007, **92**(2), 231–238.

68 B. G. Kumar, R. P. Singh and T. Nakamura, Degradation of Carbon Fiber-Reinforced Epoxy Composites by Ultraviolet Radiation and Condensation, *J. Compos. Mater.*, 2002, **36**(24), 2713–2733.

69 X. Wang, S. Kumagai, K. Kobayashi and N. Yoshimura, Degradation of Surface Contamination Performances of Outdoor Polymer Insulator Owing to Acid Rain, *IEJ. Trans.*, 1998, **118-A**, 502–508.

70 J. You, J. S. Heo, H. O. Kim and E. Kim, Direct photo-patterning on anthracene containing polymer for guiding stem cell adhesion, *Biomater. Res.*, 2016, **20**(1), 26.

71 B. Suresh, S. Maruthamuthu, M. Kannan and A. Chandramohan, Mechanical and surface properties of low-density polyethylene film modified by photo-oxidation, *Polym. J.*, 2011, **43**, 398.

72 Q. Xu, C. He, C. Xiao and X. Chen, Reactive Oxygen Species (ROS) Responsive Polymers for Biomedical Applications, *Macromol. Biosci.*, 2016, **16**(5), 635–646.

73 J. Gorham, T. Nguyen, C. Bernard, D. Stanley and R. Holbrook, Photo-induced surface transformations of silica nanocomposites, *Surf. Interface Anal.*, 2012, **44**, 1572–1581.

74 W. Wohlleben, J. Meyer, J. Muller, P. Müller, K. Vilsmeier, B. Stahlmecke and T. A. Kuhlbusch, Release from nanomaterials during their use phase: combined mechanical and chemical stresses applied to simple and multi-filler nanocomposites mimicking wear of nano-reinforced tires, *Environ. Sci.: Nano*, 2016, **3**(5), 1036–1051.

75 G. Wang, J. Yang, J. Park, X. Gou, B. Wang, H. Liu and J. Yao, Facile Synthesis and Characterization of Graphene Nanosheets, *J. Phys. Chem. C*, 2008, **112**(22), 8192–8195.

76 M. Theodore, M. Hosur, J. Thomas and S. Jeelani, Influence of functionalization on properties of MWCNT-epoxy nanocomposites, *Mater. Sci. Eng., A*, 2011, **528**(3), 1192–1200.

77 M. R. Zakaria, M. H. Abdul Kudus, H. Md. Akil and M. Z. Mohd Thirmizir, Comparative study of graphene nanoparticle and multiwall carbon nanotube filled with epoxy nanocomposites based on mechanical, thermal, and dielectric properties, *Composites, Part B*, 2017, **119**, 57–66.

78 T. Nguyen, W. Wohlleben and L. Sung, Mechanisms of Aging and Release from Weathered Nanocomposites, in *Safety of Nanomaterials along Their Lifecycle: Release, Exposure, and Human Hazards*, ed. W. Wohlleben, T. Kuhlbusch, J. Schnekenburger and C. M. Lehr, CRC Press, 2014, pp. 315–334.

79 E. Ruggiero, K. Vilsmeier, P. Mueller, S. Pulbere and W. Wohlleben, Similarity of environmental release from automotive coatings despite different composition, size, surface chemistry of (nano)forms of pigments, *Manuscript in preparation*, 2019.

80 Y. Feng, K. Lu, L. Mao, X. Guo, S. Gao and E. J. Petersen, Degradation of 14C-labeled few layer graphene via Fenton reaction: Reaction rates, characterization of reaction products, and potential ecological effects, *Water Res.*, 2015, **84**, 49–57.

81 W.-C. Hou, I. Chowdhury, D. G. Goodwin Jr, W. M. Henderson, D. H. Fairbrother, D. Bouchard and R. G. Zepp, Photochemical transformation of graphene oxide in sunlight, *Environ. Sci. Technol.*, 2015, **49**(6), 3435–3443.

82 W.-C. Hou, W. M. Henderson, I. Chowdhury, D. G. Goodwin Jr, X. Chang, S. Martin, D. H. Fairbrother, D. Bouchard and R. G. Zepp, The contribution of indirect photolysis to the degradation of graphene oxide in sunlight, *Carbon*, 2016, **110**, 426–437.

83 B. Avant, D. Bouchard, X. Chang, H. Hsieh, B. Acrey, Y. Han, J. Spear, R. G. Zepp and C. D. Knightes, Environmental fate of multiwalled carbon nanotubes and graphene oxide across different aquatic ecosystems, *NanoImpact*, 2019, **13**, 1–12.

84 Y. Han, C. D. Knightes, D. Bouchard, R. G. Zepp, B. Avant, H. Hsieh, X. Chang, B. Acrey, W. M. Henderson and J. Spear, Simulating graphene oxide nanomaterial phototransformation and transport in surface water, *Environ. Sci.: Nano*, 2019, **6**(1), 180–194.

85 C. D. Knightes, R. B. Ambrose Jr, B. Avant, Y. Han, B. Acrey, D. C. Bouchard, R. G. Zepp and T. J. Wool, Modeling framework for simulating concentrations of solute chemicals, nanoparticles, and solids in surface waters and sediments: WASP8 Advanced Toxicant Module, *Environ. Model. Softw.*, 2019, **111**, 444–458.

86 J. H. Arts, M. Hadi, M.-A. Irfan, A. M. Keene, R. Kreiling, D. Lyon, M. Maier, K. Michel, T. Petry and U. G. Sauer, A decision-making framework for the grouping and testing of nanomaterials (DF4nanoGrouping), *Regul. Toxicol. Pharmacol.*, 2015, **71**(2), S1–S27.

87 A. Oomen, E. Bleeker, P. Bos, F. van Broekhuizen, S. Gottardo, M. Groenewold, D. Hristozov, K. Hund-Rinke, M.-A. Irfan and A. Marcomini, Grouping and read-across approaches for risk assessment of nanomaterials, *Int. J. Environ. Res. Public Health*, 2015, **12**(10), 13415–13434.

88 L. Schlagenhauf, T. Buerki-Thurnherr, Y.-Y. Kuo, A. Wichser, F. Nüesch, P. Wick and J. Wang, Carbon Nanotubes Released from an Epoxy-Based Nanocomposite: Quantification and Particle Toxicity, *Environ. Sci. Technol.*, 2015, **49**(17), 10616–10623.

89 A. T. Saber, A. Mortensen, J. Szarek, I. K. Koponen, M. Levin, N. R. Jacobsen, M. E. Pozzebon, S. P. Mucelli, D. G. Rickerby, K. Kling, R. Atluri, A. M. Madsen, P. Jackson, Z. O. Kyjovska, U. Vogel, K. A. Jensen and H. Wallin, Epoxy composite dusts with and without carbon nanotubes cause similar pulmonary responses, but differences in liver histology in mice following pulmonary deposition, *Part. Fibre Toxicol.*, 2016, **13**(1), 1–20.

90 C. Pang, N. Neubauer, M. Boyles, D. Brown, N. Kanase, D. Hristozov, T. Fernandes, V. Stone, W. Wohlleben and A. Marcomini, Releases from transparent blue automobile coatings containing nanoscale copper phthalocyanine and their effects on J774 A1 macrophages, *NanoImpact*, 2017, **7**(Supplement C), 75–83.

91 J. P. Kaiser, M. Roesslein, L. Diener and P. Wick, Human Health Risk of Ingested Nanoparticles That Are Added as Multifunctional Agents to Paints: an In Vitro Study, *PLoS One*, 2013, **8**(12), e83215.

92 A. Saber, N. Jacobsen, A. Mortensen, J. Szarek, P. Jackson, A. Madsen, K. Jensen, I. Koponen, G. Brunborg, K. Gutzkow, U. Vogel and H. Wallin, Nanotitanium dioxide toxicity in mouse lung is reduced in sanding dust from paint, *Part. Fibre Toxicol.*, 2012, **9**(1), 4.

93 W. Wohlleben, S. Brill, M. Meier, M. Mertler, G. Cox, S. Hirth, B. von Vacano, V. Strauss, S. Treumann, K. Wiench, L. Ma-Hock and R. Landsiedel, On the lifecycle of nanocomposites: comparing released fragments and their in-vivo hazards from three release mechanisms and four nanocomposites, *Small*, 2011, **7**, 2384–2395.

94 W. Wohlleben, B. Hellack, C. Nickel, M. Herrchen, K. Hund-Rinke, K. Kettler, C. Riebeling, A. Haase, B. Funk and D. Kühnel, The nanoGRAVUR framework to group (nano) materials for their occupational, consumer, environmental risks based on a harmonized set of material properties, applied to 34 case studies, *Nanoscale*, 2019, **11**(38), 17637–17654.

